Materials with on-demand refractive indices in the terahertz range

Christelle Kadlec,[1] Filip Kadlec,[1,*] Petr Kužel,[1] Karine Blary,[2] and Patrick Mounaix[3]

[1]*Institute of Physics, Academy of Sciences of the Czech Republic, Na Slovance 2, 182 21 Prague 8, Czech Republic*
[2]*Institute for Electronics, Microelectronics and Nanotechnology, University of Lille, Cité Scientifique, Avenue Poincaré, BP 60069, 59652 Villeneuve d'Ascq Cedex, France*
[3]*Centre de Physique Moléculaire Optique et Hertzienne, Université Bordeaux I, 351 Cours de la Libération, 33405 Talence Cedex, France*
Corresponding author: kadlecf@fzu.cz

We demonstrate the possibility to create materials with chosen refractive indices and a strong birefringence in the terahertz range by etching of patterns with appropriate filling factors in a dielectric substrate. We show that by using deep inductive plasma etching of silicon wafers, it is possible to achieve a birefringence as high as 1.2 in an 80 μm thick layer. The resulting stacks were used as building blocks for a photonic crystal displaying sharp defect mode peaks in transmittance. © 2008 Optical Society of America

OCIS codes: 260.1440, 230.5298.

The ongoing development of new sources and applications in the terahertz range is expected to bring a demand for devices and technologies enabling an efficient manipulation of the terahertz radiation. Previous research in this direction resulted in realizing, e.g., metamaterials containing split-ring resonators with a resonance tunable by electric voltage [1] and sensitive to their environment [2], switches based on photonic crystals (PCs) containing liquid crystals [3], ferroelectric thin films [4], or terahertz filters that can operate as modulators [5].

A convenient way to obtain a tunable element is to build a one-dimensional PC consisting of a sequence of alternating layers with a high and a low refractive index and an active medium in the center giving rise to sharp tunable or switchable defect modes [6]. With an appropriate choice of materials and thicknesses, such a device works as a Fabry–Perot resonator, selecting a narrow interval of frequencies that will pass through. The optical properties of the active material in the terahertz range are influenced by an external parameter, such as laser beam illumination, temperature, or electric bias, allowing a control of transmittance at those frequencies. The properties of the device are then determined by the choice of the materials used. For an optimum tuning performance of the modulator, a high contrast between the refractive indices and a low absorption is required. Also, the active medium material should be surrounded by a medium with as low as possible refractive index (see [7] and references therein), ideally by air, which may make the assembling of the PC technically difficult. A conception of rigid easy-to-build blocks consisting of high/low refractive index bilayers is therefore highly desirable.

Only few materials exhibit birefringence in the terahertz range; the most prominent among them is lithium niobate, where its value Δn can reach up to 1.6 [8]. However, its moderate absorption and high cost make this material less convenient for mass applications. One of the common birefringent materials is wood [9], however, in this case, $\Delta n \approx 0.08$ only. Below we show that substantial birefringence in the terahertz domain can be created artificially via a metamaterial with an appropriate design as it is known from the optical range [10].

We demonstrate in this Letter a method of creating metamaterials for the terahertz range, where both the refractive index n and its birefringence can be adjusted. Our approach consists in using silicon wafers etched with a subwavelength periodicity to the depth of up to 100 μm; a similar process was used earlier in the design of a narrowband operating terahertz attenuator [11]. The thick etched layer, effectively behaving as a bulk material with modified properties, contains air, the ratio of which can be chosen by applying a specific etching mask; the mask geometry determines the refractive indices along the two principal polarization directions n_1 and n_2. Their values may range from 1 to 3.4, with $\Delta n \equiv n_2 - n_1$ up to 1.25, resulting in a high artificial birefringence. We assembled those stacks into a symmetric one-dimensional PC; this can be regarded as a matrix able to receive an active material in the center for achieving an operation allowing tuning.

To calculate the permittivity of the etched layer, we consider a rectangular unit cell [Fig. 1(a)] whose repetition constitutes the geometric pattern of the etch-
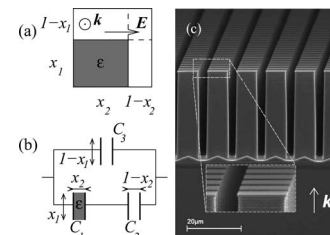

Fig. 1. (a) Scheme of a unit cell of an etched material with permittivity ε placed in air; (b) equivalent circuit applicable for evaluating its effective response. The dimensions are in relative units. (c) Scanning electron microscope picture of the structure with an array of pillars.

ing. Its lateral dimensions are much smaller than the wavelength of the terahertz waves propagating perpendicular to the unit cell plane. A rectangular part of the unit cell, with fractional dimensions $x_1 \times x_2$, is filled by a material with a permittivity ε and surrounded by air. By analogy with a system of capacitors, we can determine the effective permittivity of the unit cell and thus of the whole layer. Let us assume an incident terahertz wave propagating through the unit cell with the electric field along one of its edges. The dimensions to be taken into account to calculate the corresponding capacitances are indicated on the scheme. Within the quasi-static approximation, it is possible to replace the structure by an equivalent electric circuit, which is shown in Fig. 1(b). Its relative capacitance C directly provides access to the permittivity ε_1 of the layer parallel to the terahertz electric field; it reads

$$C = (1/C_1 + 1/C_2)^{-1} + C_3, \qquad (1)$$

with $C_1 = \varepsilon x_1 / x_2$, $C_2 = x_1/(1-x_2)$, and $C_3 = 1-x_1$. We find

$$\varepsilon_1 = 1 + \frac{x_1 x_2}{\dfrac{\varepsilon}{\varepsilon - 1} - x_2} = n_1^2, \qquad (2)$$

where n_1 is the corresponding refractive index of the layer. From Eq. (2), one can easily derive the permittivity ε_2 and the refractive index n_2 of the layer along the other edge; for reasons of symmetry, they are given by

$$\varepsilon_2 = 1 + \frac{x_1 x_2}{\dfrac{\varepsilon}{\varepsilon - 1} - x_1} = n_2^2. \qquad (3)$$

If $x_1 \neq x_2$ then $\varepsilon_1 \neq \varepsilon_2$, which corresponds to the possibility to design a birefringent material. In one extreme case, the geometry of the etched layers resembles walls—we can write, e.g., $x_1 = 1$; then, x_2 is the filling factor. Using Eqs. (2) and (3), one can show that the highest Δn occurs at $x_2 = 0.65$. For this case, using the measured refractive index of the bulk silicon $n_{Si} = 3.415$ (the absorption index is unmeasurably small), we obtain $n_1 = 1.57$, $n_2 = 2.82$, and $\Delta n = 1.25$.

The technology employed to prepare such materials consisted of an anisotropic etching of 390 μm thick undoped silicon wafers with a photoresist mask patterned in a standard photolithography process. A Surface Technology Systems equipment featuring the Bosch process, where SF_6/O_2 etching steps alternated with C_4F_8 passivation, allowed an etching rate of 5 μm/min and a high aspect ratio. Owing to underetching, the positions of etched surfaces were 1 μm away from the mask edges toward the remaining silicon. This approach produced two kinds of patterns: 7 μm $\times$ 7 μm square pillars [Fig. 1(c)] and 6 μm wide walls with pitches of 4 and 6 μm, respectively, covering useful areas of 7 mm $\times$ 7 mm. Photoresist masks were removed when the depths of pil-

lars and walls reached 60 and 80 μm, respectively. The resulting difference in width between the top and the bottom of both patterns was lower than 10%.

Considering the width of the patterns at the half depth of the etching, we find $x_1 = x_2 = 0.66$ for the pillars and $x_1 = 1$, $x_2 = 0.48$ for the walls. Within the long wavelength approximation, the expected values of the refractive indices in the terahertz domain are $n_1 = n_2 = 1.41$ for the pillars and $n_1 = 1.33$ and $n_2 = 2.47$ for the walls. We verified these values by time-domain terahertz spectroscopy. The experimental setup was based on a Ti:sapphire laser oscillator delivering 810 nm, 80 fs pulses at a 76 MHz repetition rate. The laser pulses excited an interdigitated photoconducting emitter [12], which generated linearly polarized terahertz pulses used to probe the properly oriented silicon wafers under normal incidence. A weak part of the laser beam was directed onto a 1 mm thick ⟨110⟩ cut Zn–Te crystal for electro-optic sampling of the terahertz radiation.

From the transmitted waveforms, we have calculated using Fresnel formulas the terahertz spectra of refractive indices shown in Fig. 2. As expected, the spectra are essentially flat with mean values of $n = 1.47$ for the pillars and $n_1 = 1.35$ and $n_2 = 2.45$ for the walls. These results are consistent with the calculated values, accounting for the uncertainties in the thicknesses of the etched layer and the silicon substrate, which can lead to an error of up to 10% in n. Moreover, for the wall structure, if the etched layer is misaligned by a few degrees with respect to the electric field, the measured refractive index is slightly influenced by the value of the other polarization with a more pronounced effect at lower frequencies. In all cases studied, the measured effective losses, owing to both absorption and scattering, were negligibly small (see inset of Fig. 2; the deviations from zero are owing to the experimental error). As the refractive indices can be chosen, structures of this kind could be used as antireflective layers [11,13] or half-wave plates for the terahertz range.

By rotating the birefringent sample around its surface normal we verified that the electric-field polarizations parallel and perpendicular to the walls are eigenvectors of the anisotropic medium. Namely, for any angle θ between the incident terahertz pulse polarization and the direction of walls, transmitted waveforms obey, analogously to what is shown, e. g., in Fig. 2 of [9], the relation
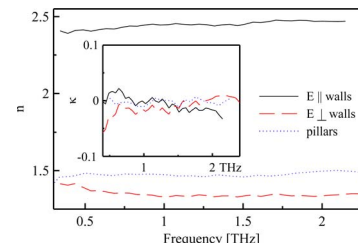

Fig. 2. (Color online) Refractive indices for different patterns of etched layers (solid and dashed curves, walls; dotted curve, pillars). n, real part; κ, index of absorption.

$$E(t,\theta) = E_{\parallel}(t)\cos^2\theta + E_{\perp}(t)\sin^2\theta, \qquad (4)$$

where $E_{\parallel}$ and $E_{\perp}$ are the terahertz pulses transmitted for $\theta = 0$ and $\theta = 90°$, respectively. In this way, we proved that the layers consisting of etched walls behave as a material with an effective anisotropy.

Finally, we gathered four of the wall-patterned wafers, the bulk silicon outside and the etched layers inside, to build a symmetric one-dimensional PC with a lattice period of $L = 0.39$ mm. The PC consisted of eight layers of wall-etched (W) and nonetched (S) Si ordered as SWSWWSWS (a twin defect in the center). We measured the terahertz signal transmitted through this structure oriented with the walls perpendicular to the electric field (effective refractive index n_1); a 280-ps-long time scan was used to achieve a fine resolution in frequency. The amplitude transmittance of the PC is shown by the solid curve in Fig. 3.

A theoretical description of the optical properties of the PC in the terahertz range can be obtained by using the transfer matrix formalism [7]. To this purpose, the PC is modeled as a sequence of layers, each of them described by a transfer matrix based on its effective optical constants. The transmittance spectrum of our PC calculated in this way, using the experimentally found values for the refractive indices and thicknesses, is shown by the dotted curve in Fig. 3. As we can see, the experimental spectra are in good agreement with the calculated ones. Nevertheless, at lower frequencies, the spectrum of experimentally obtained transmittance rises only to a level of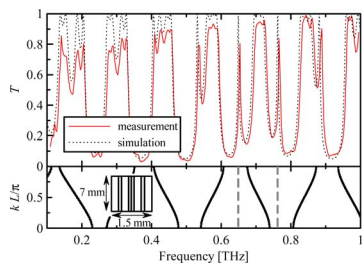 about 80% with respect to the expected values; this may be owing to an imperfect parallelism among the walls of the different layers and a residual Drudelike absorption by free carriers in the Si wafers.

Two of the observed sharp peaks (PC defect modes) appear as convenient for modulating the transmitted terahertz radiation, one at 653 GHz and one at 766 GHz; their transmittance reaches 80%, with a FWHM of 5 GHz. The positions of these peaks, as well as those of the forbidden bandgaps, can be adjusted by modifying the pattern of the etched layers. This proves the suitability of our approach for setting up on-demand building blocks of PCs in tuning applications. The real-time tunability could be obtained by inserting into the center of the structure a convenient defect material, the terahertz properties of which could be controlled externally [5,14].

Fig. 3. (Color online) Top, amplitude transmittance of the PC. The simulation is based on refractive indices $n_1 = 1.33$ and $n_{Si} = 3.415$. Bottom, band structure of an infinite defect-free PC (…SWSWSW…) and twin defect levels (dashed curves); inset, scheme of the PC.

References

1. H.-T. Chen, J. F. O'Hara, A. K. Azad, A. J. Taylor, R. D. Averitt, D. B. Shrekenhamer, and W. J. Padilla, Nat. Photonics **2**, 295 (2008).
2. Y. Sun, X. Xia, H. Feng, H. Yang, C. Gu, and L. Wang, Appl. Phys. Lett. **92**, 221101 (2008).
3. J. Li, J. He, and Z. Hong, Appl. Opt. **46**, 5034 (2007).
4. P. Kužel, F. Kadlec, J. Petzelt, J. Schubert, and G. Panaitov, Appl. Phys. Lett. **91**, 232911 (2007).
5. L. Fekete, F. Kadlec, P. Kužel, and H. Němec, Opt. Lett. **32**, 680 (2007).
6. L. Fekete, F. Kadlec, P. Kužel, and H. Němec, Opt. Express **15**, 8898 (2007).
7. P. Kužel and F. Kadlec, C. R. Acad. Sci.—Physique **9**, 197 (2008).
8. Y.-M. Sun, Z.-L. Mao, B.-H. Hou, G.-Q. Liu, and L. Wang, Chin. Phys. Lett. **24**, 414 (2007).
9. M. Reid and R. Fedosejevs, Appl. Opt. **45**, 2766 (2006).
10. O. L. Muskens, S. L. Diedenhofen, M. H. M. van Weert, M. T. Borgström, E. P. A. M. Bakkers, and J. G. Rivas, Adv. Funct. Mater. **18**, 1039 (2008).
11. S. Biber, D. Schneiderbanger, and L.-P. Schmidt, Frequenz **59**, 141 (2005).
12. A. Dreyhaupt, S. Winnerl, T. Dekorsy, and M. Helm, Appl. Phys. Lett. **86**, 121114 (2005).
13. C. Brückner, B. Pradarutti, O. Stenzel, R. Steinkopf, S. Reihemann, G. Notni, and A. Tünnermann, Opt. Express **15**, 779 (2007).
14. H. Němec, P. Kužel, L. Duvillaret, A. Pashkin, M. Dressel, and M. Sebastian, Opt. Lett. **30**, 549 (2005).